

## Article

# Influence of Dry Friction on the Dynamics of Cantilevered Pipes Conveying Fluid

Zilong Guo <sup>1,2</sup>, Qiao Ni <sup>1,2</sup>, Lin Wang <sup>1,2,\*</sup>, Kun Zhou <sup>1,2</sup> and Xiangkai Meng <sup>1,2</sup>

<sup>1</sup> Department of Engineering Mechanics, School of Aerospace Engineering, Huazhong University of Science and Technology, Wuhan 430074, China; d202080634@hust.edu.cn (Z.G.); niqiao@hust.edu.cn (Q.N.); d201780445@hust.edu.cn (K.Z.); m201971776@hust.edu.cn (X.M.)

<sup>2</sup> Hubei Key Laboratory for Engineering Structural Analysis and Safety Assessment, Wuhan 430074, China

\* Correspondence: wanglinds@hust.edu.cn

**Abstract:** A cantilevered pipe conveying fluid can lose stability via flutter when the flow velocity becomes sufficiently high. In this paper, a dry friction restraint is introduced for the first time, to evaluate the possibility of improving the stability of cantilevered pipes conveying fluid. First, a dynamical model of the cantilevered pipe system with dry friction is established based on the generalized Hamilton's principle. Then the Galerkin method is utilized to discretize the model of the pipe and to obtain the nonlinear dynamic responses of the pipe. Finally, by changing the values of the friction force and the installation position of the dry friction restraint, the effect of dry friction parameters on the flutter instability of the pipe is evaluated. The results show that the critical flow velocity of the pipe increases with the increment of the friction force. Installing a dry friction restraint near the middle of the pipe can significantly improve the stability of the pipe system. The vibration of the pipe can also be suppressed to some extent by setting reasonable dry friction parameters.

**Keywords:** dry friction; pipe conveying fluid; vibration reduction; flutter; nonlinear dynamics



**Citation:** Guo, Z.; Ni, Q.; Wang, L.; Zhou, K.; Meng, X. Influence of Dry Friction on the Dynamics of Cantilevered Pipes Conveying Fluid. *Appl. Sci.* **2022**, *12*, 724. <https://doi.org/10.3390/app12020724>

Academic Editor: Ji Wang

Received: 10 November 2021

Accepted: 1 January 2022

Published: 12 January 2022

**Publisher's Note:** MDPI stays neutral with regard to jurisdictional claims in published maps and institutional affiliations.



**Copyright:** © 2022 by the authors. Licensee MDPI, Basel, Switzerland. This article is an open access article distributed under the terms and conditions of the Creative Commons Attribution (CC BY) license (<https://creativecommons.org/licenses/by/4.0/>).

## 1. Introduction

Pipes conveying fluid have played an important role in aerospace, marine engineering, and the nuclear industry. For example, refueling aircraft through aviation refueling pipes will cause flow-induced vibrations of the pipe at higher flight speed, which will affect the practical application of pipes conveying fluid. The exploration and collection of deep-sea oil and gas require the use of kilometer-long pipes [1,2]. Under the excitation of the internal and external flows, the pipe may vibrate and deform greatly. During vibration, harsh and harmful noise may be generated and the pipe system tends to be fatigued and damaged, which may cause economic losses and serious safety accidents [3]. Therefore, the dynamic analysis and vibration control of pipes conveying fluid have attracted much attention [4–7].

Paidoussis et al. [8–10] reviewed the dynamical behavior of pipes conveying fluid under different boundary conditions and pointed out that a cantilevered pipe would be subjected to flutter instability when the internal flow velocity becomes sufficiently high. For heat-exchange bundle structures existing in the nuclear industry, beyond the onset of flutter instability, the pipe would be subjected to periodic motion and might contact the surrounding supporting plates or pipes [11–13]. In this case, the effect of contact and possible dry friction between the pipe and the surrounding structures may be pronounced. Therefore, it is inevitable to study the dynamical behavior of pipes conveying fluid with dry friction.

In the past decades, many scholars have tried to establish nonlinear dynamical models for the basic system of pipes conveying fluid. For instance, Lee et al. [14] derived the governing equations of straight pipes conveying fluid from different perspectives, which makes the longitudinal and transverse displacements of supported pipes be coupled with each other. Tan et al. [15] were focused on the application of Timoshenko beam theory

under supercritical conditions and showed that their theory is more advantageous at higher flow velocity. Sazesh et al. [16] studied the flutter velocity and dynamical behavior of a fluid-conveying pipe under distributed random excitation. On the other hand, dry friction is a typical nonlinear force, which belongs to contact nonlinearity, and it is usually characterized by piecewise linearity [17–19]. Dry friction can generate damping in some cases and was also used in the manufacturing of brake pads [20] and clutches [21]. As one of the notable works on dry friction, Ren et al. [22] applied dry friction to the support section of a simply supported beam. By using a refined model, the elastic deformation in the tangential direction of the friction surface was considered. Go et al. [23] performed a mode analysis of a beam with both ends supported under dry friction by using constraint conditions and Lagrange multipliers. Guida et al. [24] studied the dynamical behavior of a mass system under dry friction and analyzed the influence of the different parameters of dry friction on the equilibrium position of the mass system.

In this study, the stability and dynamic responses of a cantilevered pipe conveying fluid with a dry friction constraint somewhere along the length of the pipe is explored. It should be mentioned that, to the authors' knowledge, this may be the first study dedicated to the application of dry friction in non-conservative continuum system such as a cantilevered pipe conveying fluid. The equation of motion of the pipe system with dry friction is derived through the generalized Hamilton's principle. From a perspective of vibration control [25–29], by taking advantage of the energy-consumption characteristic of the dry friction, the dry friction is also expected to be effective at adjusting/controlling the stability and dynamics of the system of pipes conveying fluid.

This paper is organized as follows. In Section 2, a passive control method based on dry friction is proposed, and the equation of motion of the cantilevered pipe system with the dry friction constraint is derived through the generalized Hamilton's principle. In Section 3, the equation of motion is solved numerically based on the Galerkin method, and the typical dynamic responses of the pipe are obtained. In Section 4, the algorithm validation and convergence analysis conform the correctness of the solution method. In Section 5, the influence of the dry friction force and its installation position on the dynamics and stability of the pipe is discussed, showing that the presence of the dry friction constraint can improve the stability of the pipe and suppress the vibration of the pipe to some extent. In Section 6, some conclusions are drawn and further research directions for future research are discussed.

## 2. Theoretical Model

In this paper, the dynamical system under consideration is shown in Figure 1. The cantilevered pipe is placed vertically and connected to the ground by a dry friction restraint at  $s = s_d$ . This dry friction restraint would generate transversal friction force at the connection when the pipe is deformed at  $s_d$ . Suppose that the length of the pipe is  $L$ ; the mass per unit length of the pipe is  $m'$  the bending stiffness is  $EI$ , with  $E$  being the Young's modulus and  $I$  the moment of inertia; the Kelvin-Voigt damping coefficient of the pipe is  $E^*$ , and the acceleration of gravity is  $g$ . There is a fluid passing through the slender pipe. The mass per unit length of the fluid is  $M$ , and the average flow velocity is  $U$ . For simplicity, it is assumed that the pipe moves in a plane. The lateral displacement of the cantilevered pipe along the  $y$  axis is represented by  $y(s,t)$ , which is a function of the curvilinear coordinate  $s$  and time  $t$ .

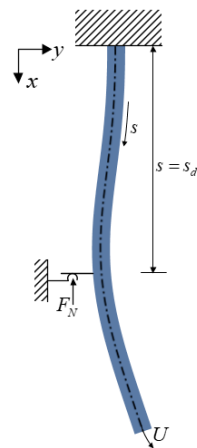


**Figure 1.** Schematic diagram of the cantilevered pipe with a dry friction restraint.

The following assumptions are introduced: (1) the pipe centerline is inextensible; (2) the fluid is incompressible; (3) the moment of inertia and shear deformation of the pipe are ignored; (4) the fluid velocity is uniform and constant; (5) the pipe strain is small, although its lateral displacement may be large. Now introduce the generalized Hamilton’s principle [9]:

$$\delta \int_{t_1}^{t_2} (T - V) dt + \int_{t_1}^{t_2} \delta W_f dt = \int_{t_1}^{t_2} \{ MU[(\partial r_L / \partial t) + U\tau_L] \cdot \delta r_L \} dt \tag{1}$$

where the Lagrangian of the system includes the kinetic energy  $T$  and potential energy  $V$  of the cantilevered pipe system, and  $W_f$  represents virtual work done by the dry friction. The term on the right side of the Equation (1) represents the influence on the system when the fluid flows into and out of the pipe. The position vector and tangential direction of the pipe are denoted as  $r$  and  $\tau$ , respectively, and they are given by

$$r = xi + yj, \tau = \frac{\partial x}{\partial s}i + \frac{\partial y}{\partial s}j \tag{2}$$

where  $i$  and  $j$  are the unit vectors in the  $x$ - and  $y$ -direction, respectively. In addition, the velocities of the pipe and the fluid are as

$$v_p = \frac{\partial r}{\partial t} = \dot{x}i + \dot{y}j, v_f = (\dot{x} + Ux')i + (\dot{y} + Uy')j \tag{3}$$

The total kinetic energy of the pipe and the fluid is expressed as

$$T = T_p + T_f = \frac{1}{2}m \int_0^L v_p^2 ds + \frac{1}{2}M \int_0^L v_f^2 ds \tag{4}$$

The potential energy due to the deformation of the pipe is

$$V = \frac{1}{2}EI \int_0^L \kappa^2 ds = \frac{1}{2}EI \int_0^L \left( \frac{\partial^2 y / \partial s^2}{\sqrt{1 - (\partial y / \partial s)^2}} \right)^2 ds \tag{5}$$

The dry friction force exists as a non-conservative force of the system, and its work is given by

$$W = - \int_0^{y(s_d, t)} F(y) dy(s_d, t) \tag{6}$$

Substituting Equations (4)–(6) into Equation (1), one can obtain the governing equation for the cantilevered pipe with dry friction:

$$\begin{aligned}
 & (m + M)\ddot{y} + 2MU\dot{y}'(1 + y'^2) + E^*I\dot{y}'''' + (m + M)gy'(1 + \frac{1}{2}y'^2) \\
 & + y'' \left[ MU^2(1 + y'^2) - (m + M)g(L - s)(1 + \frac{3}{2}y'^2) \right] \\
 & + y' \int_0^s (m + M)(\dot{y}'^2 + y'\ddot{y}') ds + EI \left[ y''''(1 + y'^2) + 4y'y''y'''' + y''^3 \right] \\
 & - y'' \left[ \int_s^L \int_0^s (m + M)(\dot{y}'^2 + y'\ddot{y}') ds ds + \int_s^L (2MUy'y' + MU^2y'y'') ds \right] \\
 & + F(\dot{y})\delta(s - s_d) = 0
 \end{aligned} \tag{7}$$

where the over-dot and prime denote the partial differentiation with respect to  $t$  and  $s$ , respectively.  $\delta(s - s_d)$  is the Dirac delta function, and  $s_d$  denotes the location of the dry friction restraint.  $F(\dot{y})$  is the dry friction force acting on the pipe, and the direction is related to the lateral velocity at the location  $s_d$ . When the stick and sliding occur between the contact surfaces, the dry friction force can simulate the real situation well.

It is well-known that dry friction force is produced by applying constant pressure to the friction interfaces. When the flow velocity exceeds a certain value, the pipe may generate flutter instability and result in motions. Therefore, the classic coulomb friction model is suitable to approximate the effect of dry friction. This model considers the dynamic friction, ignoring the difference between static and dynamic situations, which is suitable for the situation where adhesion rarely occurs. Thus, the coulomb friction model considers dry friction as a discontinuous nonlinear load. The dry friction is proportional to the normal pressure acting on the friction surfaces, and is independent of the contact area. The direction of the friction force is opposite to the movement direction of the friction surfaces. The expression of the friction force is given by [17].

$$F(\dot{y}) = \mu F_N \text{sign}[\dot{y}(s_d, t)] \tag{8}$$

where  $\mu$  is the friction coefficient;  $F_N$  is the normal pressure, and  $\text{sign}[\dot{y}(s_d, t)]$  denotes the sign function. It is noted that  $\text{sign}[\dot{y}(s_d, t)]$  is equal to 1 when  $\dot{y}(s_d, t)$  is positive and otherwise it is equal to  $-1$ .

Now the following non-dimensional parameters are introduced

$$\begin{aligned}
 \xi &= \frac{s}{L}, \eta = \frac{y}{L}, \tau = \sqrt{\frac{EI}{m+M}} \frac{t}{L^2}, u = \sqrt{\frac{M}{EI}} UL, \beta = \frac{M}{m+M}, \\
 \alpha &= \sqrt{\frac{I}{E(M+m)}} \frac{E^*}{L^2}, \gamma = \frac{m+M}{EI} L^3 g, f_n = \frac{\mu F_N L^2}{EI}
 \end{aligned} \tag{9}$$

Substituting Equation (9) into Equation (7), we can obtain the non-dimensional governing equation as follows

$$\begin{aligned}
 & \alpha \dot{\eta}'''' + \eta'''' + \ddot{\eta} + \gamma \eta'(1 + \frac{1}{2}\eta'^2) + \eta'' \left[ u^2(1 + \eta'^2) - \gamma(1 - \xi)(1 + \frac{3}{2}\eta'^2) \right] \\
 & + \eta'''' \eta'^2 + 4\eta' \eta'' \eta'''' + \eta''^3 + 2u \sqrt{\beta} \dot{\eta}'(1 + \eta'^2) + \eta' \int_0^\xi (\dot{\eta}'^2 + \eta' \ddot{\eta}') d\xi \\
 & - \eta'' \left[ \int_\xi^1 \int_0^\xi (\dot{\eta}'^2 + \eta' \ddot{\eta}') d\xi d\xi + \int_\xi^1 (2u \sqrt{\beta} \eta' \dot{\eta}' + u^2 \eta' \eta'') d\xi \right] \\
 & + f_n \text{sign}[\dot{\eta}(\xi_d, \tau)] \delta(\xi - \xi_d) = 0
 \end{aligned} \tag{10}$$

### 3. Numerical Solution

In this section, the Galerkin method is used to discretize Equation (10). We take the suitable  $N$ -order modes of the cantilevered beam for truncation approximation. Then the lateral displacement of the pipe can be written as

$$\eta(\xi, \tau) = \sum_{r=1}^N \varphi_r(\xi) q_r(\tau) = \varphi q \tag{11}$$

where  $\varphi_r(\xi)$  is the non-dimensional modal function of a cantilevered beam, and  $q_r(\tau)$  is the generalized coordinate of the corresponding discrete system. Thus,  $\varphi$  and  $q$  denote  $1 \times N$  and  $N \times 1$  vectors, respectively.

By substituting Equation (11) into Equation (10), using the orthogonality of modal functions, then multiplying each term of the equation by  $\varphi^T$  and integrating from 0 to 1, the following ordinary differential equations can be obtained:

$$(M_l + M_{nl})\ddot{q} + (C_l + C_{nl})\dot{q} + (K_l + K_{nl})q + \varphi^T(\xi_d)f_n \text{sign}[\varphi(\xi_d)\dot{q}] = 0 \quad (12)$$

where  $M_l$  and  $M_{nl}$  are mass matrices;  $C_l$  and  $C_{nl}$  are the damping matrices;  $K_l$  and  $K_{nl}$  are the stiffness matrices. The subscripts  $l$  and  $nl$  represent linear terms and nonlinear terms, respectively.  $\dot{q} = (\dot{q}_1, \dot{q}_2, \dots, \dot{q}_N)^T$  and  $\ddot{q} = (\ddot{q}_1, \ddot{q}_2, \dots, \ddot{q}_N)^T$  are the generalized coordinate velocity and generalized coordinate acceleration, respectively.

We can solve Equation (12) numerically by using the Runge-Kutta method to obtain the dynamic responses of the pipe system.

#### 4. Algorithm Validation and Convergence Analysis

Before starting calculations, it is necessary to check the correctness of the proposed algorithm. For this purpose, by setting the dry friction force to 0, the bifurcation diagram of the tip-end response of the cantilevered pipe without dry friction is obtained, as shown in Figure 2, for a pipe system with  $\alpha = 0$ ,  $\beta = 0.142$  and  $\gamma = 18.9$  [30]. In the calculations,  $N$  is temporarily chosen to be  $N = 4$ , which will be analyzed in the convergence analysis. The constructing rule of the bifurcation diagram is: for a given flow velocity, after the responses of the pipe become steady, the tip-end displacement of the pipe is recorded when the corresponding velocity of movement becomes 0. Thus, as the flow velocity continues to increase, all the tip-end displacement amplitudes of the pipe can be recorded.

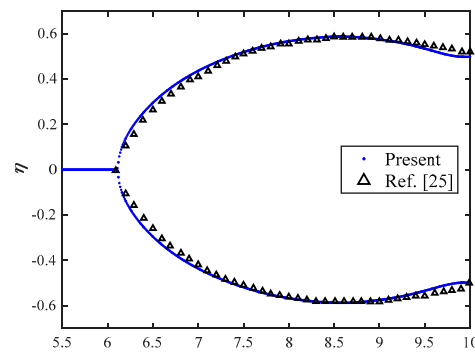


**Figure 2.** Bifurcation diagrams for the tip–end responses of a pipe system without dry friction, for  $\alpha = 0$ ,  $\beta = 0.142$ , and  $\gamma = 18.9$ .

From Figure 2, it is seen that the critical flow velocity for flutter instability and the vibration amplitudes of the pipe predicted using  $N = 4$  agree very well with the classical results given by Paidoussis [30], showing the reliability of the algorithm used in this study.

The cantilevered pipe is a type of infinite dimensional continuous system. In the application of the Galerkin method, therefore, it is necessary to examine the convergence of the modal truncation approximation, to determine the suitable value of  $N$ .

In order to observe the effect of dry friction on the stability of the system more conveniently, the gravity is ignored in the following analysis. The key system parameters are chosen to be:  $\alpha = 0.001$ ,  $\beta = 0.213$ ,  $\gamma = 0$ ,  $f_n = 0.3$ , and  $\xi_d = 0.5$ . The modal truncation number  $N$  is chosen as 4, 5 or 6. The bifurcation diagrams of the tip-end responses of the pipe with different modal numbers are given in Figure 3. It is seen that, when  $N$  is given different values, the three bifurcation diagrams are very similar, showing that the results of  $N = 4$  are acceptable. In addition, when the dry friction was installed at several typical positions, several other bifurcation diagrams for the pipe’s responses have been obtained

by taking more extensive calculations. Again, it was found that the utilization of  $N = 4$  is reliable for predicting the dynamic responses of the pipe. Due to the similarity of these additional bifurcation diagrams, the corresponding results will not be given here. To reduce calculations, therefore, we will take  $N = 4$  in all of the following calculations.

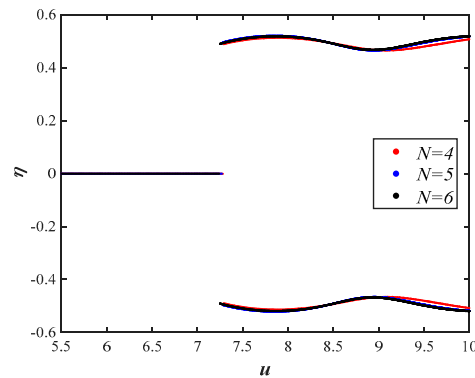


**Figure 3.** Convergence analysis of the Galerkin’s truncation approximation.

### 5. Results

In this section, we will discuss the influence of two dry friction parameters on the critical flow velocity for flutter instability and the response amplitudes of the pipe when the dry friction force ( $f_n$ ) and the installation positions of the dry friction ( $\zeta_d$ ) are varied. Based on this, we can examine the effect of the dry friction constraint on the dynamics of the fluid-conveying pipe system.

#### 5.1. Effect of Friction Force $f_n$

For certain friction surfaces, the values of the friction force mainly depend on the normal pressure acting on the friction surfaces. In this subsection, we will explore the effect of different friction forces on the stability of the pipe system. Thus, the friction force  $f_n$  is respectively taken as 0.1, 0.3, and 0.5 for analysis, with  $\zeta_d = 0.5$ . The other two key parameters of the pipe system are  $\alpha = 0.001$  and  $\beta = 0.213$ . The results of the bifurcation diagrams are shown in Figure 4. The blue and red dots represent the bifurcation diagrams without dry friction and with dry friction, respectively.

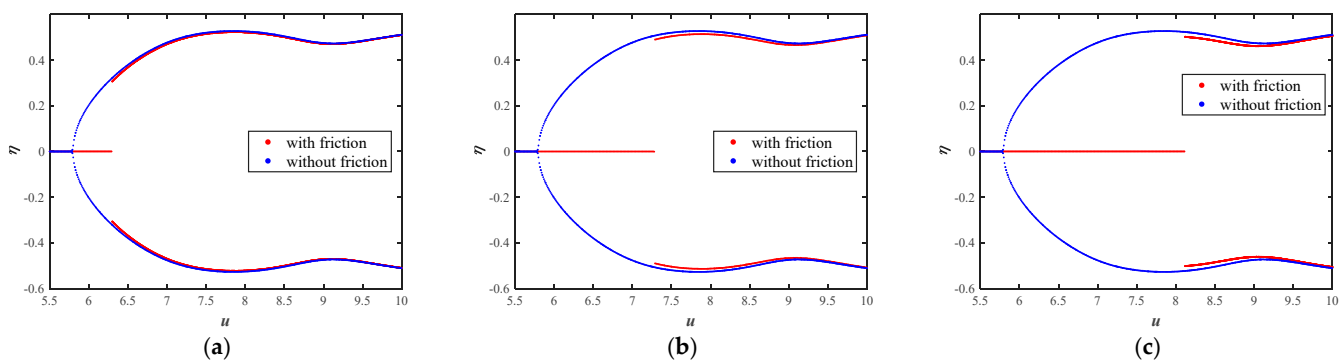


**Figure 4.** Bifurcation diagrams for the tip–end responses of the pipe with different dry friction forces when  $\alpha = 0.001$ ,  $\beta = 0.213$ , and  $\zeta_d = 0.5$ : (a)  $f_n = 0.1$ ; (b)  $f_n = 0.3$ ; (c)  $f_n = 0.5$ .

It is seen from Figure 4 that the dimensionless critical flow velocity of the pipe for flutter instability is about 5.78 without dry friction. When the applied dry friction force is 0.1, as shown in Figure 4a, the critical flow velocity of the pipe system will increase to 6.29. Moreover, the dry friction has almost no effect on the vibration amplitude of the pipe when the pipe system becomes unstable. It is also seen that, when the flow velocity is slightly

higher than the critical value, the displacement amplitude at the end of the pipe has a jump with a discontinuous change, which may be related to the applied dry friction force because the expression of the dry friction force is a discontinuous function in mathematical form. When the direction of the lateral velocity at  $\xi_d$  changes sign, the sign of the friction force will become opposite, and thus, a jump change in the bifurcation diagram occurs.

It can be seen from Figure 4b that when the friction force increases to 0.3, the critical flow velocity of the pipe system will increase to 7.28. The results given in Figure 4c are for  $f_n = 0.5$ , showing that the critical flow velocity increases to 8.11. Therefore, as the friction force acting on the pipe increases, the critical flow velocity of the pipe system will also increase, which is beneficial to improving the stability of the system. It can also be understood that applying a friction force to the cantilevered pipe is somehow equivalent to adding a loose constraint or a form of support to the pipe. The larger the friction force, the greater the energy consumed by the system can be achieved. Hence, the stability of the pipe with dry friction would be enhanced.

When the flow velocity in the pipe exceeds the critical value, the pipe would produce relatively large-amplitude vibration. Figure 5 shows the time history curve, oscillation shapes, and phase portrait of the response of the pipe when the flow velocity is 7.5 under the condition defined in Figure 4b. It can be seen from Figure 5a that the vibration of the pipe is steady in this case, and the amplitude is about 0.5. Figure 5b shows the oscillation shapes of the cantilevered pipe at this flow velocity, indicating that the response of the pipe mainly contains the first- and second-mode components of a cantilevered beam. The phase diagram given in Figure 5c shows that the pipe vibrates in the form of a limit cycle motion.

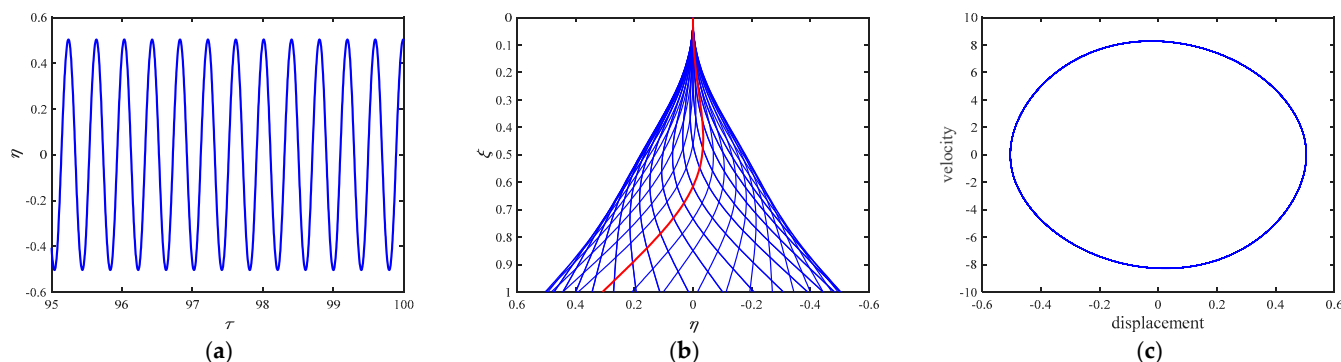


**Figure 5.** Dynamic response of the pipe with dry friction when  $u = 7.5$ : (a) Time history curve of the tip–end of the pipe; (b) oscillation shapes of the pipe; (c) phase portrait of the tip–end of the pipe.

### 5.2. Effect of Installation Position $\xi_d$

Next, we will discuss the effect of the installation position of the dry friction restraint on the stability of the pipe system. The location parameter  $\xi_d$  is set to be 0.3, 0.5, 0.7, and 0.9. The other key parameters are chosen to be:  $\alpha = 0.001$ ,  $\beta = 0.213$ , and  $f_n = 0.5$ . The obtained bifurcation diagrams are shown in Figure 6. When the installation position of the dry friction restraint is  $\xi_d = 0.3$ , it can be seen that the system is subjected to flutter instability at  $u = 7.72$ . As the flow velocity is in the range of  $[7.73, 7.87]$ , compared with the pipe without dry friction, the displacement amplitude at the free end of the pipe is significantly reduced. When the flow velocity continues to increase, however, the effect of dry friction on the vibration amplitude of the pipe is not pronounced.

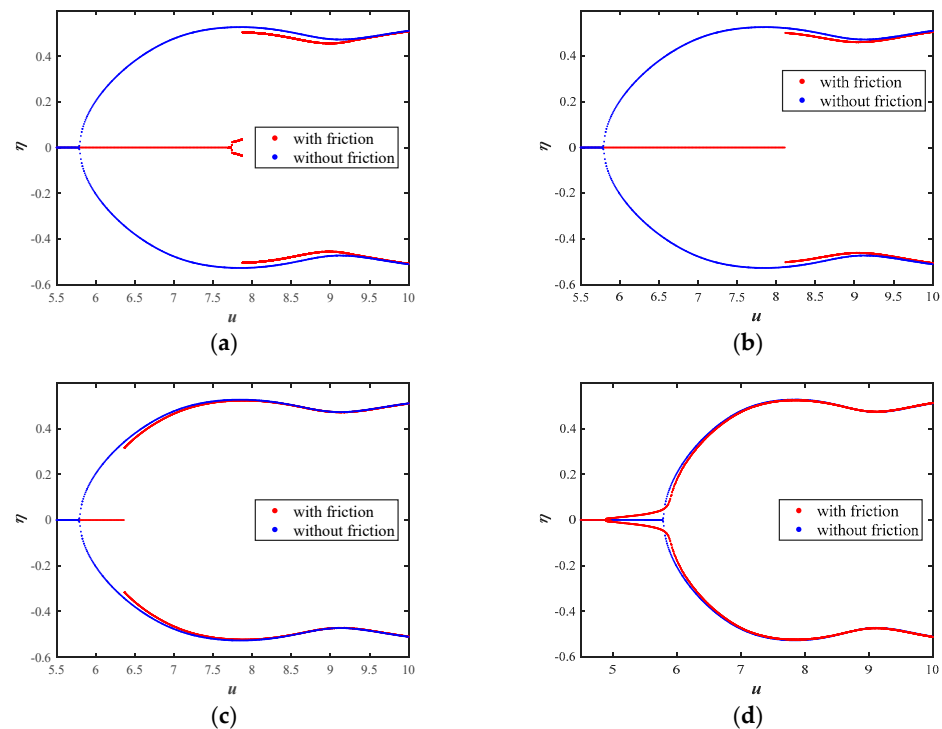


**Figure 6.** Bifurcation diagrams for the tip–end responses of the pipe for different installation positions, with  $\alpha = 0.001$ ,  $\beta = 0.213$ , and  $f_n = 0.5$ : (a)  $\zeta_d = 0.3$ ; (b)  $\zeta_d = 0.5$ ; (c)  $\zeta_d = 0.7$ ; (d)  $\zeta_d = 0.9$ .

When the installation position is  $\zeta_d = 0.5$ , the critical flow velocity increases to 8.11, as shown in Figure 6b. However, when the installation position is  $\zeta_d = 0.7$ , Figure 6c shows that the critical flow velocity of the pipe system is reduced to 6.36. As the installation position  $\zeta_d$  continues to increase to 0.9, it is found that the critical flow velocity of the pipe system decreases obviously if compared with the pipe without the dry friction, indicating that the stability of the pipe is weakened in this case. For  $\zeta_d = 0.9$ , the pipe begins to lose stability at the flow velocity  $u = 4.89$ , which is much lower than the critical flow velocity  $u_{cr} = 5.78$  for a pipe without dry friction. As the flow velocity continues to increase, the displacement amplitude at the tip-end of the pipe would gradually increase. Therefore, the result for  $\zeta_d = 0.9$  shows that the application of the dry friction might be detrimental to the stability of the pipe system in some special cases.

In order to better observe the dynamical behavior of the pipe after flutter instability, we further calculated the time history curve of the pipe with  $\zeta_d = 0.3$  and  $u = 7.8$ , as shown in Figure 7a. It is noted that the pipe vibrates periodically, but the vibration amplitude of the pipe with the dry friction constraint is much smaller than that of the pipe without dry friction, again, showing that the application of dry friction restraint can suppress the vibration of the pipe. The phase portrait and power spectral density (PSD) curve of the pipe with dry friction at this flow velocity are given in Figures 7b and 7c, respectively. The phase portrait is shown as an ellipse-like shape. It is noted that the phase portrait of Figure 7b is not a strictly periodic motion. This is because that the maximum displacements of the pipe in this case might fluctuate slightly, resulting in a relatively disordered PSD curve. However, since the fluctuation of the displacement of the pipe is relatively small, the pipe may be still considered to be in a periodic-like motion.

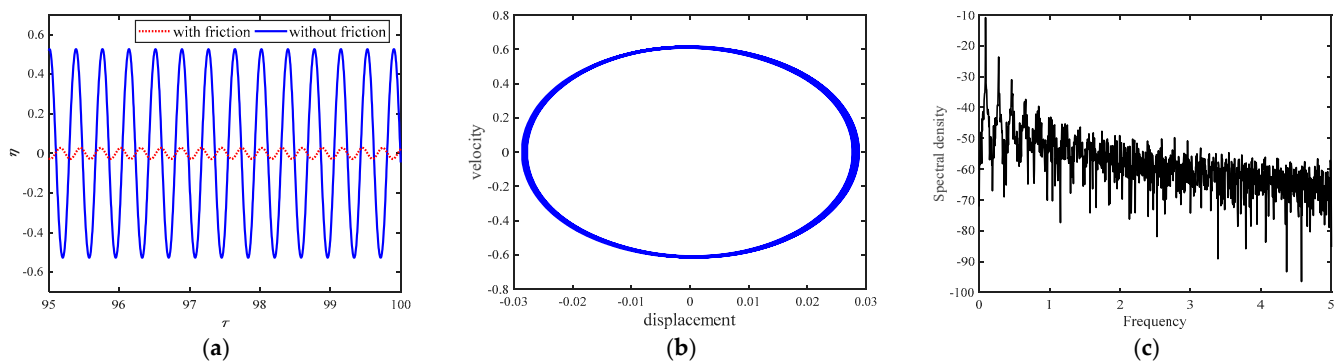


**Figure 7.** Dynamic response of the pipe with dry friction at the tip—end of the pipe when  $u = 7.8$  and  $\zeta_d = 0.3$ : (a) time history curve; (b) phase portrait; (c) PSD curve.

Thus, through numerical calculations, we have analyzed the influence of dry friction on the stability and vibration response of the pipe. It can be seen that the critical flow velocity of the system can be greatly increased by installing a suitable dry friction support, which provides a new idea for the passive control method in the dynamical system of pipes conveying fluid. As a result, the dry friction force and the installation position have a great influence on the overall dynamical behavior of the pipe, and the vibration amplitude of the pipe can be greatly suppressed in certain ranges of flow velocity. Therefore, these two important system parameters of dry friction can be adjusted to improve the stability of the pipe system.

## 6. Conclusions

In this study, a dry friction constraint is introduced in the passive vibration control of cantilevered pipes conveying fluid for the first time. The equation of motion of the cantilevered pipe with dry friction constraint is derived first through generalized Hamilton's principle. Then, the equation of equation is discretized based on the Galerkin method, and the dynamic response of the pipe with dry friction constraint is obtained by using a Runge-Kutta algorithm.

Through extensive calculations, the dynamic responses of the pipe under different dry friction parameters are analyzed, focusing on the effect of the friction force and the installation position of the dry friction restraint. The results show that the critical flow velocity can be greatly increased in many cases when the dry friction restraint is introduced. Thus, the greater dry friction can significantly improve the stability of the cantilevered pipe. At the same time, the dynamic response of the pipe can be also greatly affected by the installation positions of the dry friction restraint. When the installation position is near the middle of the pipe length, the critical flow velocity can be significantly increased. If, however, the installation position is close to the free end of the pipe, the additional friction restraint may decrease the critical flow velocity, which will cause the pipe to be more prone to instability.

In future studies, it is expected to extend the basic idea of this study to the vibration control of pipes conveying fluid, from the single-point dry friction mode proposed in this work to an optimized multi-point dry friction mode. In particular, according to the modal shape characteristics of the unstable modes of the cantilevered pipe, it is also expected to design some special multi-point dry friction constraints for improving the control effect. Indeed, the control methods based on the idea of nonlinearities including dry friction are becoming an attractive topic in the field of dynamics and vibration control of fluid-loaded structures such as pipes conveying fluid.

**Author Contributions:** Writing—original draft preparation, validation, Z.G.; writing—review and editing, conceptualization, supervision, L.W.; funding acquisition, L.W. and Q.N.; methodology, formal analysis, visualization, K.Z. and X.M. All authors have read and agreed to the published version of the manuscript.

**Funding:** This research was funded by the National Natural Science Foundation of China (Nos. 11972167 and 12072119) and the Fundamental Research Funds for the Central Universities (No. 2021yjsCXCY041).

**Institutional Review Board Statement:** Not applicable.

**Informed Consent Statement:** Not applicable.

**Data Availability Statement:** Not applicable.

**Conflicts of Interest:** The authors declare no conflict of interest.

## References

1. Liu, J.; Guo, X.Q.; Wang, G.R.; Liu, Q.Y.; Fang, D.; Huang, L.; Mao, L.J. Bi-nonlinear vibration model of tubing string in oil & gas well and its experimental verification. *Appl. Math. Model.* **2020**, *81*, 50–69. [[CrossRef](#)]
2. Wan, M.; Yin, Y.X.; Liu, J.; Guo, X.Q. Active boundary control of vibrating marine riser with constrained input in three-dimensional space. *Nonlinear Dyn.* **2021**, *106*, 2329–2345. [[CrossRef](#)]
3. Tang, D.M.; Dowell, E.H. Chaotic oscillations of a cantilevered pipe conveying fluid. *J. Fluids Struct.* **1988**, *2*, 263–283. [[CrossRef](#)]
4. Szmids, T.; Przybylowicz, P. Critical flow velocity in a pipe with electromagnetic actuators. *J. Theor. Appl. Mech.-Pol.* **2013**, *51*, 487–496.
5. Dai, H.L.; Wang, L. Dynamics and stability of magnetically actuated pipes conveying fluid. *Int. J. Struct. Stab. Dyn.* **2016**, *16*, 1550026. [[CrossRef](#)]
6. Khajepour, S.; Azadi, V. Vibration suppression of a rotating flexible cantilever pipe conveying fluid using piezoelectric layers. *Lat. Am. J. Solids Struct.* **2015**, *12*, 1042–1060. [[CrossRef](#)]
7. Lyu, X.; Chen, F.; Ren, Q.; Tang, Y.; Ding, Q.; Yang, T. Ultra-thin Piezoelectric Lattice for Vibration Suppression in Pipe Conveying Fluid. *Acta Mech. Solida Sin.* **2020**, *33*, 770–780. [[CrossRef](#)]
8. Paidoussis, M.P.; Li, G.X. Pipes Conveying Fluid: A Model Dynamical Problem. *J. Fluids Struct.* **1993**, *7*, 137–204. [[CrossRef](#)]
9. Semler, C.; Li, G.X.; Paidoussis, M.P. The non-linear equations of motion of pipes conveying fluid. *J. Sound Vib.* **1994**, *169*, 577–599. [[CrossRef](#)]
10. Paidoussis, M.P. *Fluid-Structure Interactions: Slender Structures and Axial Flow*, 2nd ed.; Elsevier Academic Press: San Diego, CA, USA, 2014; Volume 1.
11. Wang, Y.K.; Wang, L.; Ni, Q.; Dai, H.; Yan, H.L.; Luo, Y. Non-planar responses of cantilevered pipes conveying fluid with intermediate motion constraints. *Nonlinear Dyn.* **2018**, *93*, 505–524. [[CrossRef](#)]
12. Liu, L.; Li, B.; Zhang, J.S.; Li, P.F.; Xiao, X.X.; Xing, Y.; Tan, U.X. Dynamic simulation for beam to beam frictionless contact using a novel region detection algorithm. *Comput. Methods Appl. Mech. Eng.* **2021**, *385*, 114025. [[CrossRef](#)]
13. Zakirichnaya, M.M.; Rubtsov, A.V.; Kulakov, P.A.; Galiullina, N.J. The assessment of stressed-deformed state of tube bundle of the heat-exchange apparatus with the fixed pipe grids. *J. Phys. Conf. Ser.* **2020**, *1679*, 042050. [[CrossRef](#)]
14. Lee, S.I.; Chung, J. New non-linear modelling for vibration analysis of a straight pipe conveying fluid. *J. Sound Vib.* **2002**, *254*, 313–325. [[CrossRef](#)]
15. Tan, X.; Mao, X.Y.; Ding, H.; Chen, L.Q. Vibration around non-trivial equilibrium of a supercritical Timoshenko pipe conveying fluid. *J. Sound Vib.* **2018**, *428*, 104–118. [[CrossRef](#)]
16. Sazesh, S.; Shams, S. Vibration analysis of cantilever pipe conveying fluid under distributed random excitation. *J. Fluids Struct.* **2019**, *87*, 84–101. [[CrossRef](#)]
17. Olsson, H.; Strm, K.J.; Wit, C.; Gfvert, M.; Lischinsky, P. Friction Models and Friction Compensation. *Eur. J. Control* **1998**, *4*, 5517–5522. [[CrossRef](#)]
18. Berger, E. Friction modeling for dynamic system simulation. *Appl. Mech. Rev.* **2002**, *55*, 25–32. [[CrossRef](#)]
19. Wit, C.C.D.; Olsson, H.; Astrom, K.J.; Lischinsky, P. A new model for control of systems with friction. *IEEE Trans. Automat. Control* **1995**, *40*, 419–425. [[CrossRef](#)]
20. Kinkaid, N.M.; O'Reilly, O.M.; Papadopoulos, P. Automotive disc brake squeal. *J. Sound Vib.* **2003**, *267*, 105–166. [[CrossRef](#)]
21. Miyasato, H.H.; Segala Simionatto, V.G.; Junior, M.D. On the interaction between rigid discs and rotating damped contact elements. *Mech. Res. Commun.* **2021**, *111*, 103644. [[CrossRef](#)]
22. Ren, Y.S.; Qin, H.Z.; Zhao, Z.L. Nonlinear vibration analysis of a beam with dry friction at the supports. *Mech. Res. Commun.* **1999**, *26*, 83–90. [[CrossRef](#)]
23. Go, Y.J.; Kim, Y.H.; Chang, H.G. An analysis of the behavior of a simply supported beam with a dry friction damper attached. *Appl. Acoust.* **1998**, *55*, 31–41. [[CrossRef](#)]
24. Guida, D.; Nilvetti, F.; Pappalardo, C.M. Instability induced by dry friction. *Int. J. Mech.* **2009**, *3*, 44–51.

25. Zhou, K.; Xiong, F.R.; Jiang, N.B.; Dai, H.L.; Yan, H.; Wang, L.; Ni, Q. Nonlinear vibration control of a cantilevered fluid-conveying pipe using the idea of nonlinear energy sink. *Nonlinear Dyn.* **2018**, *95*, 1435–1456. [[CrossRef](#)]
26. Miguélez, M.H.; Rubio, L.; Loya, J.A.; Fernández-Sáez, J. Improvement of chatter stability in boring operations with passive vibration absorbers. *Int. J. Mech. Sci.* **2010**, *52*, 1376–1384. [[CrossRef](#)]
27. Zeng, Y.; Ding, H.; Du, R.; Chen, L. A suspension system with quasi-zero stiffness characteristics and inerter nonlinear energy sink. *J. Vib. Control* **2022**, *28*, 143–158. [[CrossRef](#)]
28. Wong, W.O.; Tang, S.L.; Cheung, Y.L.; Cheng, L. Design of a dynamic vibration absorber for vibration isolation of beams under point or distributed loading. *J. Sound Vib.* **2007**, *301*, 898–908. [[CrossRef](#)]
29. Li, Q.; Liu, W.; Lu, K.; Yue, Z. Nonlinear Parametric Vibration of a Fluid-Conveying Pipe Flexibly Restrained at the Ends. *Acta Mech. Solida Sin.* **2019**, *33*, 327–346. [[CrossRef](#)]
30. Paidoussis, M.P.; Semler, C. Non-linear dynamics of a fluid-conveying cantilevered pipe with a small mass attached at the free end. *Int. J. NonLinear Mech.* **1998**, *33*, 15–32. [[CrossRef](#)]